Dual-Mode EPR Study of New Signals from the S_3-State of Oxygen-Evolving Complex in Photosystem II†

Takaya Matsukawa,‡ Hiroyuki Mino,§ Daiki Yoneda,‡ and Asako Kawamori*,‡

Faculty of Science, Kwansei Gakuin University, Uegahara 1-1-155, Nishinomiya 662-8501, Japan, and Photosynthesis Research Laboratory, The Institute of Physical and Chemical Research (RIKEN), Wako, Saitama 351-0198, Japan

Received August 3, 1998; Revised Manuscript Received January 25, 1999

ABSTRACT: The light-induced new EPR signals at $g = 12$ and 8 were observed in photosystem II (PS II) membranes by parallel polarization EPR. The signals were generated after two flashes of illumination at room temperature, and the signal intensity had four flashes period oscillation, indicating that the signal origin could be ascribed to the S_3-state. Successful simulations were obtained assuming $S = 1$ spin for the values of the zero-field parameters, $D = \pm 0.435 \pm 0.005$ cm^{-1} and $E/D = -0.317 \pm 0.002$. Orientation dependence of the $g = 12$ and 8 signal intensities shows that the axial direction of the zero-field interaction of the manganese cluster is nearly parallel to the membrane normal.

Oxygen evolution in plant photosynthesis is accomplished by a protein pigment complex called Photosystem II (PS II[1]). The function of oxygen evolution is known to be catalyzed by a manganese cluster located on the donor side of PS II. Cofactors of three protein complexes, calcium (Ca^{2+}) and chloride (Cl^-), are also essential for this function (*1*−*4*). On the donor side, a photo-oxidized P680 is reduced by an electron donated from Y_Z (a tyrosine electron donor in PS II). The Y_Z oxidized is then rereduced by the electron from the manganese cluster in the oxygen-evolving complex (OEC). On the acceptor side, an electron is transferred through pheophytin to the primary (Q_A) and secondary (Q_B) electron acceptor quinones, and then to Photosystem I (PS I). Successive abstraction of four electrons from OEC was carried out by absorption of light by P680 four times and results in evolution of molecular oxygen.

The oxidizing center cycles through a series of the five oxidation states, called S-states with S_n ($n = 0-4$), n denoting the number of stored oxidizing equivalents. The S_4-state is a transient state because it rapidly decays to the S_0-state by releasing molecular oxygen (*5*, *6*). The S_1-state is most stable of five oxidation states in the dark at room temperature. The S_2- and S_3-states are unstable and decay back to the S_1-state. With decreasing temperature of illumination, the formation of higher S-states is blocked; the transitions S_1- to S_2-state and S_2- to S_3-state are blocked at about 80 and 210 K, respectively (*7*).

EPR signals of the Mn cluster can be observed for the S_0- and S_2-state at a low temperature by a conventional mode EPR. Several EPR species have been observed in the S_2-state. One of the S_2-state EPR signals is centered at $g = 2$ with an overall line width of about 1600 G (*8*). The signal exhibits 18−20 partially resolved hyperfine lines separated by 85−90 G and has been called the multiline signal (*8*). The other S_2-state EPR signal is centered at $g = 4.1$ with a peak-to-trough line width of about 400 G (*9*−*12*). Upon illumination of PS II samples at 140 K, the $g = 4.1$ signal was induced preferentially to the multiline (*10*, *11*). This signal thus formed converts to the multiline signal when annealed at 200 K in the dark. The two signals are generated concurrently upon illumination at 200 K (*10*). The presence of various alcohols with low molecular weights (ethylene glycol, ethanol, and methanol) suppresses the formation of the $g = 4.1$ signal upon illumination at 200 K and complementarily enhances the multiline signal intensity (*12*, *13*). Recently, Boussac et al. have reported that the new signals at $g = 10$ and 6 can be observed by a conventional EPR, which were assigned to $m_S = \pm 5/2$ and $\pm 3/2$ transitions in an $S = 5/2$ spin system (*14*).

Parallel polarization EPR ($\mathbf{H}_1 // \mathbf{H}_0$, microwave field is parallel to the static field) can be used to detect a $\Delta m_S = 0$ transition. This technique has been often used to investigate integer spin systems and will supply new information that cannot be obtained by a conventional EPR method ($\mathbf{H}_1 \perp \mathbf{H}_0$, perpendicular mode) only. The S_1-state signal centered at $g = 4.9$ with a peak-to-trough width of about 600 G was found by Dexheimer and Klein using the parallel polarization EPR (*15*). Further studies have characterized that the S_1-state signal was attributed to the excited triplet states of weakly antiferromagnetically coupled manganese ions, with $J = -0.87$ cm^{-1} (*16*). Recently, the S_1-state signal with a hyperfine structure was reported in the PS II particles lacking 17 and 23 kDa (*17*).

S_0-state EPR signals have been found by two groups, which have hyper fine structures similar to the multiline

† This work was supported by Hyogo Science and Technology Association.

* Corresponding author. Telephone: 81-798-54-6383. Fax: 81-798-51-0914. E-mail: kawamori@kwansei.ac.jp.

‡ Kwansei Gakuin University.

§ The Institute of Physical and Chemical Research (RIKEN).

[1] Abbreviations: PS II, photosystem II; OEC, oxygen-evolving complex; Chl, chlorophyll; Y_D, redox-active tyrosine 161 of D2 protein; Y_Z, redox-active tyrosine 161 of D1 protein; P680, the reaction center chlorophyll; MES, 2-morpholinoethanesulfonic acid; EDTA, ethylenediaminetetraacetic acid; DCMU, 3-(3,4-dichlorophenyl)-1,1-dimethylurea; PPBQ, phenyl-1,4-benzoquinone; EPR, electron paramagnetic resonance; XANES, X-ray absorption near edge structure.

10.1021/bi9818570 CCC: $18.00
Published on Web 03/12/1999

signal in the S_2-state but with a broader overall width (*18*, *19*). The signal was ascribed to the antiferromagnetically coupled $S = {}^1/_2$ system in a ground state (*20*).

These reports suggest that the manganese is oxidized directly during the transitions from S_0 to S_1 and S_1 to S_2. X-ray absorption near edge structure (XANES) studies also indicated that the S-state transitions involve changes in the valence state of the Mn cluster (*21*, *22*).

In this work, we have observed new EPR signals. The new signals were generated after two turnovers from the S_1-state and showed a period four oscillation by flash illumination at room temperature, indicating that the new signals originate from the S_3-state. The signals were attributed to an $S = 1$ spin system, suggesting that the manganese in OEC might be oxidized during the transition from the S_2- to S_3-state.

MATERIALS AND METHODS

Oxygen-evolving PS II membranes were prepared from market spinach by the method of Kuwabara and Murata (*23*) and stored in liquid N_2 until use. The following procedures were conducted in complete darkness or under a dim green safe light unless otherwise noted. PS II membranes suspended in a final buffer medium containing 0.4 M sucrose, 15 mM NaCl, 5 mM $MgCl_2$, 1 mM EDTA, and 50 mM Mes/NaOH (pH 6.0) were collected by centrifugation at 35000*g* for 25 min, and transferred into EPR tubes with 4 mm inner diameter. The final chlorophyll concentration was approximately 20 mg/mL for continuous or 3.5 mg of Chl/mL for flash illumination, respectively. PPBQ (1 mM) is supplemented to the PS II samples for flash experiment.

To measure angular dependence of the EPR spectra, we dried the PS II membranes suspended in the same buffer solution on pieces of Mylar sheets for 15 h at 277 K under N_2 stream with 90% humidity (*24*). Pieces (6−8) of piled Mylar sheets with about 3×15 mm^2 were inserted into an EPR tube. A disordered powder sample was obtained from the oriented membranes with the Mylar sheets removed.

Manganese was removed from the membrane with 0.8 M Tris/HCl at pH 8.0 and stirring on ice for 30 min under room light at a concentration with 0.3 mg of Chl/mL (*25*).

All of the samples were dark-adapted for 2 h before illumination to ensure 100% of the S_1-state. The samples were illuminated for 10 min at 235 K by a 500 W tungsten bromide lamp through a 10 cm thick water filter and immediately trapped in liquid N_2. A cryocool tip immersed in an ethanol bath was used for regulation of illumination temperature between 200 and 254 K. A Nd:YAG laser (Continuum Surelite I) with 220 mJ, 5 ns pulse at the wavelength of 532 nm was used for flash illumination. The same quantity (70 μL) of PS II membranes was loaded into 7 different sample tubes for 0−6 flashes of illumination.

EPR measurements were carried out on a Bruker ESP300E X-band spectrometer equipped with an ER4116 DM X-band dual-mode resonator. The microwave frequency can be changed to resonate with the perpendicular TE_{102} or the parallel TE_{012} mode. An Oxford 900 continuous flow cryostat was used to regulate sample temperatures from 5 to 20 K. An Oxford Helium pumping system with a ESR910 continuous flow cryostat was used below 5 K. The sample temperature was indicated by a gold−iron (0.07 atom %) chromel thermocouple that was calibrated by a carbon−glass resistor inserted into a sample tube containing the buffer medium. The temperature below 4.2 K was measured by the vapor pressure inside the cryostat when liquid helium was pumped. The value of the vapor pressure has been also calibrated by the carbon−glass resistor in the similar way. At 5.7 K, higher- and lower-temperature data were connected. The temperature dependence of the $Y_D^\bullet$ signal intensity was measured as an internal standard in the perpendicular mode to confirm the accuracy of temperature measurements before measurements in the parallel polarization mode (*16*).

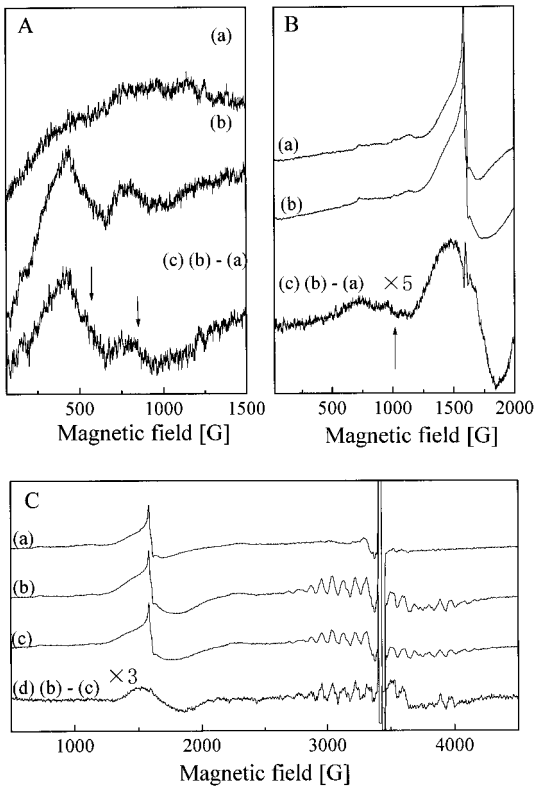

FIGURE 1: EPR signals observed in untreated PS II membranes by parallel (A) and perpendicular (B) polarized microwave modes: the spectra of dark-adapted membranes (a), after illumination for 10 min at 235 K (b), and light-minus-dark difference spectra (c). The arrow in panel B shows an allowed transition EPR, which is remarkable only over the low-field range sweep. The spectra (C) observed by the perpendicular mode over the wide-field range show the multiline and $g = 4.1$ signals for dark-adapted (a), illumination at 200 (b) and 235 K (c), and subtraction (d) = (b) − (c). About 30% less multiline intensity for 235 K illumination was observed than for 200 K illumination (b). EPR conditions for parallel mode: microwave frequency, 9.34 GHz; microwave power, 3.2 mW; field modulation amplitude, 8 G at 100 kHz; scan time, 168 s; time constant, 0.1 s; temperature, 5.5 K; data accumulation, 16 scans. EPR conditions for perpendicular mode: microwave frequency, 9.57 GHz; data accumulation, 4 scans in panel B and 1 scan in panel C. Others are the same as in panel A.

The angle between the magnetic field and the membrane normal (**n**) was monitored by the line shape of the $Y_D^\bullet$ signal (*24*). The EPR spectra in the S_3-state were obtained by the subtraction of the spectrum for the S_1-state or the S_2-state that was obtained by the illumination for 10 min at 200 K.

RESULTS

Figure 1 shows parallel (A) and perpendicular polarized (B, C) EPR spectra in the photosystem II membranes

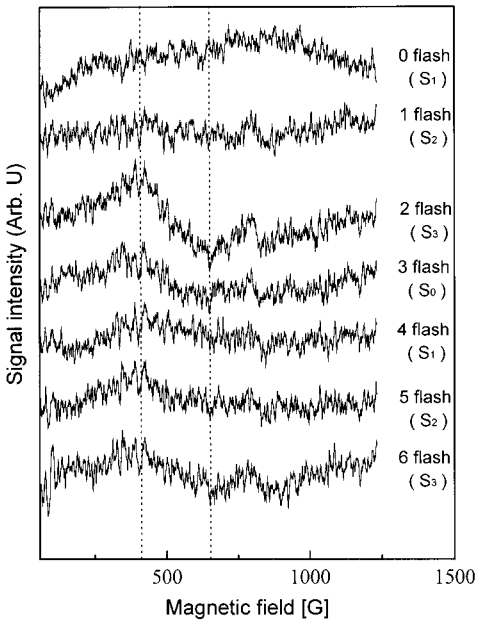

FIGURE 2: Flash dependence of parallel polarization EPR signals observed in the PS II with 1 mM PPBQ added. Flash illumination was carried out at room temperature. Zero-flash (S_1-state) spectrum at the uppermost line was subtracted from each spectrum of flash-illuminated samples. EPR conditions are the same as those described in Figure 1 except for the data accumulation of 64 scans.

illuminated for 10 min at 235 K. The light (panel A, trace b) minus dark (panel A, trace a) difference spectrum (panel A, trace c) reveals two EPR signals $g_{ob} = 12$ and 8 with their peak-to-peak widths of about 300 and 200 G, respectively, in the parallel polarized mode. g_{ob} is referred to the observed field position to discriminate g-value used for simulation. The S_1-state signal ($g_{ob} = 4.9$) disturbed the new signals negligibly because it has much broader width and less intensity at the different resonance positions. The $g_{ob} = 12$ and 8 signals have revealed the maximum intensity by about 245 K illumination but no remarkable intensity below 200 K illumination (data not shown). A broad signal was also detected at $g_{ob} \approx 6.7$ with a width of 700 G in the perpendicular mode as shown in Figure 1 (panel B, trace c), although the overlap from the $g = 4.1$ signal made it difficult to separate the $g_{ob} \approx 6.7$ signal only. Panel C shows the spectra observed over the wider field range including the multiline and $g = 4.1$ signals in the same sample. The multiline intensity for illumination at 235 K (c) was estimated to be less by 30 ± 5% (d) than for illumination at 200 K (b) and about 52 ± 5% for illumination at 245 K (data not shown). The $g = 4.1$ signal intensity in the 235 K illuminated sample was also less than that in the multiline by the same amount as shown in trace d.

Figure 2 shows the flash-dependent parallel mode EPR spectra recorded in the untreated PS II membranes. The spectrum of 0th flash at the upper most line was subtracted from each spectrum below. The signals at $g = 12$ and 8 magnetic field strength were not observed on the first flash. Hereafter we omit the suffix "ob" in g_{ob} except for when it is necessary. However, the signals appeared on the second flash, and gradually decreased with the third to fifth flashes. The signal intensity slightly increased again on the sixth flash. The multiline spectrum appeared on the first flash, decreased at the second to fourth flashes, and recovered at the fifth flash (not shown). The periodicity of four was

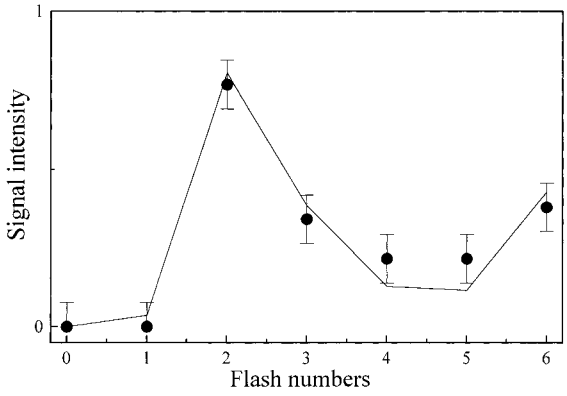

FIGURE 3: Relative yield of the parallel polarization EPR signal observed at $g = 12$ (circles) estimated from the peak height between two dashed lines in Figure 2. The relative intensities of the $g = 12$ signals are drawn by the solid line simulated by Kok's model with the assumed values for double-hit $\alpha = 0.03$, miss hit $\beta = 0.16$, and the initial condition of 100% S_1-state.

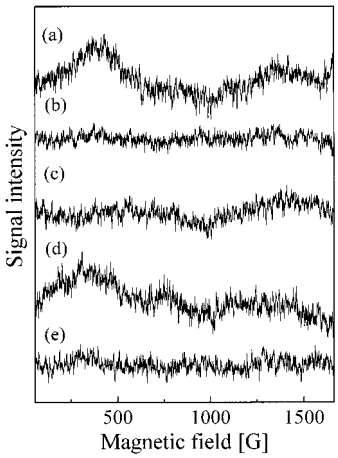

FIGURE 4: Parallel mode EPR signals of several treated samples: (a) the spectrum for untreated PS II membranes; (b) in the presence of 50 μM DCMU; (c) in the presence of 3% methanol; (d) supplemented by 50 vol % glycerol; and (e) in Tris-treated PS II membranes. EPR signals were observed in 235 K illuminated minus 273 K dark-adapted difference spectra. EPR conditions are the same as those described in Figure 1.

observed in both $g = 12$, 8 and multiline intensities in the same samples.

The flash number dependence of the EPR intensities was plotted in Figure 3, where the signal intensities were evaluated by the peak-to-peak height for the $g = 12$ signal. The flash number dependence of the period 4 indicates that the signals in the parallel mode originate from the S_3-state in OEC. The straight line shows the simulated intensity by Kok's model assuming miss hit $\beta = 0.16$ and double hit $\alpha = 0.03$. The maximum intensity of $g = 12$ signal obtained by flash experiment was estimated to be about 2.6 times that of the 235 K illuminated sample. The S_3-state advancement by the second flash was estimated from the amount of the multiline intensity in the 235 K illuminated sample to be at most 80%.

Figure 4 shows the effect of various treatments of the PS II membranes on the signals at $g = 12$, 8 produced by 235 K illumination for 10 min. The $g = 12$, 8 signals were not detected in the presence of 50 μM DCMU (trace b), which is consistent with the result of flash number dependence. In the presence of 3% methanol, the signals were not induced

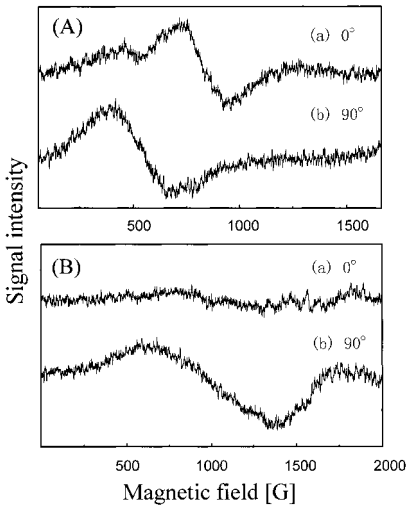

FIGURE 5: Angular dependence of the EPR spectra in oriented PS II membranes observed by parallel (A) and perpendicular (B) modes. The angles between the external magnetic field direction and the membrane normal are 0° (A) and 90° (B), respectively. The spectra of the S_2-state produced by 200 K illumination have been subtracted from each spectra as a background after annealing at 235 K to diminish the $g = 4.1$ signal. EPR conditions are the same as those described in Figure 1.

(trace c). Trace d shows the spectra observed in the 50% glycerol added PS II membranes, where the same signal shape as in the control PS II shown in trace a was observed. Trace e shows that no signal was observed in Tris-treated PS II, indicating that the signal can be ascribed to the donor side including the Mn cluster.

Figure 5 shows EPR signals observed on parallel (A) and perpendicular (B) polarized modes in oriented PS II membranes by illumination for 12 min at 235 K. Traces a and b in both modes show the results of subtraction by the spectra for the S_2-state in which the same sample was annealed at 235 K for 10 min in the dark after the 200 K illumination. This dark annealing diminished the $g = 4.1$ signal intensity so as to isolate the $g \approx 6.7$ signal. The two signals at $g = 12, 8$ show different orientation dependence on the magnetic field direction as shown for 0° and 90°, respectively. The signal intensity at $g = 12$ is maximal for the angle of 90°, and that at $g = 8$ is maximal for 0°. The angular dependence of the signal intensities for both g-values was plotted in Figure 6. In Figure 5B a broad signal was detected at $g = 6.7$ for the angle of 90° in the perpendicular mode, while the intensity of the signal decreased for the angle 0°. However, overlapping of the $g = 4.1$ signal could not be eliminated completely and made it difficult to isolate the $g = 6.7$ component only from the spectra in the low-field region. Therefore, the estimation of the signal intensity was not accurate on this mode.

Figure 7 shows the EPR signals observed in the powder sample on the parallel (A) and perpendicular (B) modes, which show the same line shape as in Figure 1 but with much higher intensity because of more concentration. Background subtraction has been done as mentioned for Figure 1. Spectral simulation will be carried out on these powder spectra.

We assume that the signals can be assigned to a metal center with high spin number system, because the large effective g-value cannot be assigned to an ordinary free radical. Out of a large number of alternatives, we consider

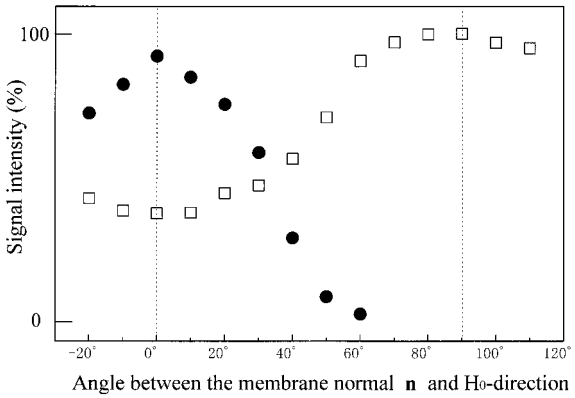

FIGURE 6: Angular dependence of the $g = 12$ and 8 signal intensities observed in oriented PS II membranes on the parallel polarization mode. The intensities were estimated by the peak-to-peak height for each spectrum $g = 12$ (squares) and 8 (circles).

only the case where the signal results from an isolated spin multiplet. The spin Hamiltonian for $S \geq 1$ spin system is given by a molecular coordinate system.

$$H = \beta \mathbf{H_0} \cdot \mathbf{g} \cdot \mathbf{S} + D[S_z^2 - {}^1/_3 S(S+1)] + E(S_x^2 - S_y^2) \quad (1)$$

where D and E are zero-field splitting parameters, and **g** and β are the **g** tensor and the value of the Bohr magneton, respectively. To calculate the transition probability for detection by the parallel polarization mode at a given resonance frequency ν_0 of 9.34 GHz, we carried out diagonalization of eq 1 for varying values of input parameters; the magnetic field strength H_0, and its direction (θ, ϕ) relative to the zero-field z-axis for trial values of D and E. An isotropic g-value of 2.0 is assumed, as there is no large anisotropy of g factor for a manganese ion (*26*). The transition matrixes between two levels j and k connected by S_z' for parallel and S_x' for perpendicular modes, respectively, were calculated, where primes on spin components are refered to the laboratory coordinate system.

We could satisfactorily simulate the line shape obtained on the parallel mode using the values of zero-field parameters; $D = \pm 0.435 \pm 0.005$ cm^{-1} and $E/D = -0.317 \pm 0.002$ with a Gaussian line width $\Delta\nu = 200$ MHz. In Figure 7 the lines show the simulation spectra for $S = 1$ spin system. The discrepancy of the simulation spectrum at the high field side of $g = 6.7$ signal in the perpendicular mode can be ascribed to the overlapping of the $g = 4.1$ signal. The computer simulation shows that the $g = 12, 8$ signals can be assigned to the components with magnetic field direction perpendicular and parallel, respectively, to the membrane normal (**n**) and the $g = 8$ signal arises from the zero-field z-component, indicating that the zero-field z-axis is along the membrane normal (**n**). The above parameters fit also well with the experimental spectral positions and intensities for the orientations 0° and 90° in Figure 5.

In Figure 8 the inset shows $g = 12, 8$ signals observed at different temperatures. With increasing temperature, the signal intensity decreases with no appreciable change in the line shape. The signals almost disappear below the noise level above 20 K. Temperature dependence of the $g = 12, 8$ signal intensities was plotted versus inverse temperature in Figure 8. To avoid saturation, microwave power was set to 0.8 and 0.2 mW, respectively, above and below 5 K. The plot of the

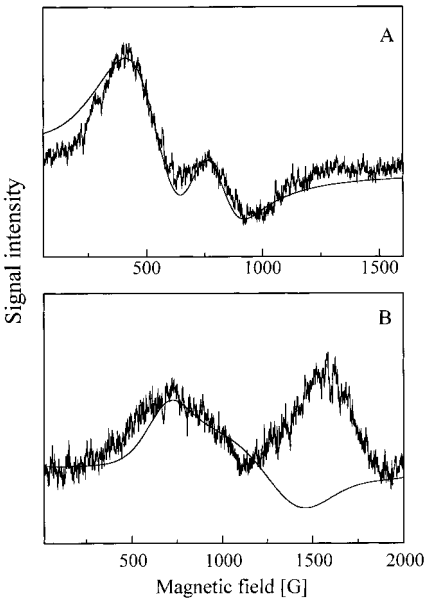

FIGURE 7: EPR signals observed by parallel (A) and perpendicular (B) polarized microwave field after illumination of a powder sample for 12 min at 235 K. Each spectrum has been subtracted by the S_1-state one as described in Figure 1. The solid line displays the result of simulation using the following parameters: $S = 1$, $g = 2.0$, $D = \pm 0.435$ cm^{-1}, $E/D = -0.317$, and $\Delta\nu = 200$ MHz. See text for details.

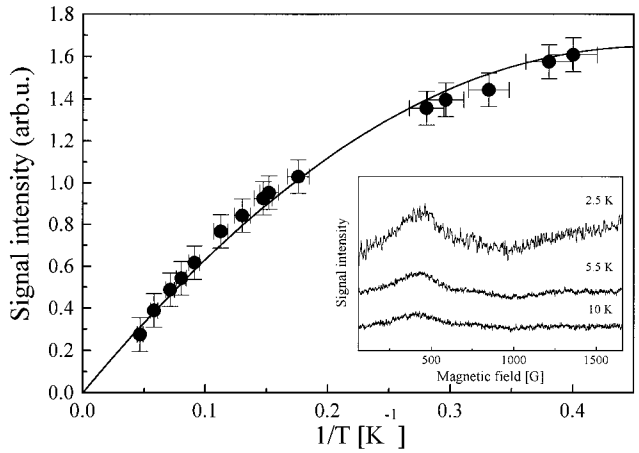

FIGURE 8: Temperature dependence of the $g = 12$ and 8 signal intensity in the disordered powder sample. The signals above and below 5 K were detected at microwave powers of 0.8 and 0.2 mW, respectively, and normalized by $Y_D^\bullet$ intensity. The powers used for S_3 and $Y_D^\bullet$ (0.01 μW) signals at 2 K are confirmed to be nonsaturating. Vertical and horizontal bars indicate error ranges for the estimation of signal intensity and temperature, respectively. The curve is fitted to eq 2 in text; for $S = 1$, $E_S = 2.4$ cm^{-1}. The spectra in the inset show the observed temperature variation. EPR conditions are the same as those described in Figure 1 except for the above-described microwave power.

peak ($g = 12$) to trough ($g = 8$) intensity deviates from the Curie law to lower values below 5 K. The non-Curie law behavior suggests that the signals arise from a low-lying excited state.

DISCUSSION

The present study demonstrated that the illumination of the untreated PS II membrane induced new EPR signals with $g = 12$ and 8 in the parallel mode and $g = 6.7$ in the perpendicular mode. The signals were generated after two flashes of illumination at room temperature and the signal intensity had the four flash period oscillation, indicating that the signal origin could be ascribed to the S_3-state. For low-temperature illumination the S_3 advancement was at most ~50%. The two new signals can be explained by the anisotropic component of the $S = 1$ spin system by the angular dependence of their intensity shown in Figure 6.

Overlapping of the $g = 4.1$ signal makes it difficult to measure and simulate the $g = 6.7$ component. The possibility that the $g = 6.7$ signal in the perpendicular mode may be attributed to another center with $S = 1$ spin cannot be excluded completely. However, the signal in perpendicular mode could be simulated by using the same parameters as those in parallel mode. Tentatively, the signal in the perpendicular mode can be assigned to the other transition of the same $S = 1$ spin system.

There might be other possibilities that the signals might not originate from $S = 1$. In a $S \geq 2$, only the *z*-component described in eq 1 has the resonance at the low field as discussed in ref *27*. However, there were two signal components in the parallel mode as shown in Figure 1A. Therefore the possibility of an $S \geq 2$ was excluded to interpret these two spectra. A half-integer spin system ($S \geq {}^3/_2$) might give a low-field signal; however, we could not obtain the parameters satisfied with the experimental spectra. Only the assumption of $S = 1$ spin system under the condition of $g = 2$ in eq 1 gave the satisfactory simulation to fit the observed spectra.

The oxidation state of the S_2-state Mn cluster is assumed to be Mn(III)-3Mn(IV) by XANES study (*1*−*4*) or 3Mn(III) + Mn(IV) by the EPR simulation (*28*). One of the four manganese or the redox-active residues such as histidine is proposed to be oxidized during the transition from the S_2- to the S_3-state (*22*). If the redox-active organic residue were oxidized, the exchange coupling between the Mn cluster in the S_2-state with $S = {}^1/_2$ and the organic residue with $S = {}^1/_2$ should result in the disappearance of the multiline signal for an $S = 1$ spin system to be created. In this case, the interaction between the manganese responsible to the multiline signal ($S = {}^1/_2$, $g = 2$) and the organic residue ($S = {}^1/_2$, $g = 2$) will have the resonance line at $g_{ob} = 2$. Therefore, this possibility should be excluded from the result, $g_{ob} = 12$, 8, in this work. Another possibility is that the $S = {}^1/_2$ organic radical and the $S = {}^3/_2$ manganese state may couple to produce $S = 1$ and 2 states. In this case, a suitable fitting might be found for the excited $S = 1$ state with $S = 2$ as a ground state. The possibility of other choices of couplings in a multi-spin system cannot be completely neglected. Therefore, the simulation here may be considered to be a tentative one and a more detailed study will be necessary to determine the oxidation state of the S_3-state.

The temperature dependence of the $g = 12$, 8 signal intensity showed the non-Curie law behavior, indicating that the signals arise from an excited state. The observed temperature dependence can be fitted for a state of spin of *S*, by neglecting the contribution from Zeeman and zero-field interactions,

$$I(T) = \{I_0/T\}(2S + 1)\exp(-E_s/kT)/\sum_j(2S_j + 1)\exp(-E_j/kT) \quad (2)$$

where I_0 is a constant to be fitted. Using $E_s = 2.4$ cm^{-1} for

the ground state with $S = 0$, and 0.8 cm^{-1} for the ground state with $S = 2$, respectively, the signal intensity could be fitted to the observed temperature dependence. The magnetic susceptibility of PS II observed at room temperature shows an increasing tendency with flash illuminations (*29*), which suggest that the higher-energy levels with nonzero spin numbers contribute to the susceptibility. At a low temperature only low-lying states contributed to the EPR intensity. Therefore, it is difficult to deduce the exchange scheme of the Mn cluster as shown in other systems (*30*) from the value derived in this work.

Methanol addition to the PS II membranes suppresses the formation of the $g = 4.1$ signal upon illumination at 200 K and complementarily enhances the multiline signal intensity as observed for the S_2-state (*12*). Thus methanol may lead to a change of exchange coupling between Mn atoms (*13*), resulting in the disappearance of the $g = 12$, 8 signals as shown in Figure 4c. The similar effect has been reported in the S_1-state, in which methanol inhibits the formation of the S_1-state signal (*16*). Not only the oxidation state but also a change in the second coordination area of manganese atoms (*31*) might lead to the change in the exchange scheme for each S-state. The value of $E_S = 2.4 \pm 0.2$ cm^{-1}, derived from the temperature dependence of $g = 12$, 8 signal intensity, happens to be similar to the value of $E_S = -2J = 1.74$ cm^{-1} for the S_1-state signal (*16*), showing that a combination of various exchange interactions might produce the similar temperature dependence for the S_2- and S_3-states. Detailed model simulations satisfying the EPR characteristics over the S_0- to S_3-states will be necessary to elucidate the magnetic structure of the manganese cluster.

REFERENCES

1. Debus, R. J. (1992) *Biochim. Biophys. Acta 1102*, 269−352.
2. Yachandra, V. K., Sauer, K., and Klein M. P. (1996) *Chem. Rev. 96*, 2927−2950.
3. Britt, R. D. (1996) in *Oxygenic Photosynthesis: The Light Reactions* (Ort, D. R., and Yocum, C. F., Eds.) pp 137−164, Kluwer Academic Publishers, New York.
4. Adelroth, P., Lindberg, K., and Andreasson, L. E. (1995) *Biochemistry 34*, 9021−9027.
5. Kok, B., Forbush, B., and Mcgloin, M. (1970) *Photochem. Photobiol. 11*, 457−475.
6. Joliot, P., Barbieri, G., and Chabaud, R. (1969) *Photochem. Photobiol. 10*, 309−329.
7. Styring, S., and Rutherford, A. W. (1988) *Biochim. Biophys. Acta 933*, 378−387.
8. Dismukes, G. C., and Siderer, Y. (1981) *Proc. Natl. Acad. Sci. U.S.A. 78*, 274−248.
9. de Paula, J. C., Innes J. B., and Brudvig, G. W. (1985) *Biochemistry 24*, 8114−8120.
10. Zimmermann, J.-L., and Rutherford, A. W. (1984) *Biochim. Biophys. Acta. 767*, 160−167.
11. Casey, J. L., and Sauer, K. (1984) *Biochim. Biophys. Acta 767*, 21−28.
12. Zimmermann, J.-L., and Rutherford, A. W. (1986) *Biochemistry 25*, 4609−4615.
13. Pace, R. J., Smith, P., Bramley, R., and Stehlik, D. (1991) *Biochim. Biophys. Acta 1058*, 161−170.
14. Boussac, A., Un, S., Horner, O., and Rutherford, A. W. (1998) *Biochemistry 37*, 4001−4007.
15. Dexheimer, S. L., and Klein, M. P. (1992) *J. Am. Chem. Soc. 114*, 2821−2826.
16. Yamauchi, T., Mino, H., Matsukawa, T., Kawamori, A., and Ono, T. (1997) *Biochemistry 36*, 7520−7526.
17. Campbell, K. A., Gregor, W., Pham, D. P., Peloquin, J. M., Debus. R. J., and Britt, R. D. (1998) *Biochemistry 37*, 5039−5045.
18. Åhrling, K. A., Peterson, S., and Styring, S. (1997) *Biochemistry 36*, 13148−13152.
19. Messinger, J., Nugent, J. H. A., and Evans, M. C. W. (1997) *Biochemistry 36*, 11055−11060.
20. Åhrling, K. A., Peterson, S., and Styring, S. (1998) *Biochemistry 37*, 8115−8120.
21. Ono, T., Noguchi, T., Inoue, Y., Kusunoki, M., Matsushita, T., and Oyanagi, H. (1992) *Science 258*, 1335−1337.
22. Roelofs, T. A., Liang, W., Latimer, M. J., Cinco, R. M., Rompel, A., Andrews, J. C., Sauer, K., Yachandra, V. K., and Klein M. P. (1996) *Proc. Natl. Acad. Sci. U.S.A. 93*, 3335−3340.
23. Kuwabara, T., and Murata, N. (1982) *Plant Cell Physiol. 23*, 533−539.
24. Rutherford, A. W. (1985) *Biochim. Biophys. Acta 807*, 189−201.
25. Mino, H., and Kawamori, A. (1994) *Biochim. Biophys. Acta 1185*, 213−220.
26. Pecoraro, V. L. (1988) *Photochem. Photobiol. 48*, 249−264.
27. Mino, H., Kawamori, A., Matsukawa, T., and Ono, T-a. (1998) *Biochemistry 37*, 2795−2799.
28. Zheng, M., and Dismukes, G. C. (1996) *Inorg. Chem.* 35, 3307−3319.
29. Sivaraja, M., Philo, J. S., Lary, J., and Dismukes, G. C. (1989) *J. Am. Chem. Soc. 111*, 3221−3225.
30. Bencini, A., and Gatteschi, D. (1990) *Electron Paramagnetic Resonance of Exchange Coupled System*, Springer-Verlag, Berlin, Germany.
31. Randall, D. W., Gelasco, A., Caudle, M. T., Pecoraro, V. L., and Britt, R. D. (1997) *J. Am. Chem. Soc. 119*, 4481−4491.

BI9818570